International Journal of Researches in Biosciences, Agriculture & Technology | January 2014 Issue-2, Volume-1 | ISSN No. (Online) 2347-517X

CRYSTALLITE SIZE EFFECT OF FE DOPING ON SnO_2 NANOPARTICLES

A. S. Lanje[1,*], S. J. Sharma[2]

[1]*Department of Electronics, Dr. Ambedkar College, Chandrapur-442 401,*
[2]*Department of Electronics, R .T. M. Nagpur University, Nagpur-441 001,*

Abstract

Iron (Fe) doped SnO_2 nanoparticles are prepared using co-precipitation method from $SnCl_2$ and $FeSO_4$ precursors and subsequent heat-treatment at 600 °C. These nanoparticles crystallise in tetragonal system. The unit cell volume increases slightly with Fe^{2+} doping indicating substitution of Sn^{4+} sites by Fe^{2+} ions. With increasing Fe^{2+} concentration, the peaks in X-ray diffraction pattern become broad because of strain effect produced from substitution of smaller ionic radius Sn^{4+} (0.69 Å) by large one Fe^{2+} (0.77 Å). The average crystallite size was found to decrease from 21 nm to 11 nm as Fe^{2+} concentration increases from 0 to 10 at %. In Transmission Electron Microscopy (TEM) study of pure SnO_2, the particles are spherical in shape and particle size is found to be 25 nm, which is close to 21 nm from XRD study. Its Selected Area Electron Diffraction (SAED) confirms the tetragonal system. In infrared study, a broad peak centered around 650 cm^{-1} was observed due to Sn-O/Fe-O vibration.

Keywords: Nanoparticles, strain, doping, co-precipitation.

*Corresponding author's e-mail: amrut.lanje@gmail.com

1. Introduction

High-transparency semiconductors such as SnO_2 have potential applications in flat panel displays and gas sensors, etc. [1–8]. Bulk SnO_2 has wide band-gap (E_g) of 3.6 eV. In the last few years, transition metal (TM) doped semiconducting oxides in order to induce room temperature (RT) ferromagnetism has become an interesting topic. This kind of materials, named dilute magnetic semiconductors (DMS), is of great interest as potential materials for spintronic applications [9-11]. Many results have been reported on Co, Fe, Ni or Mn doped TiO_2 [9] and SnO_2 systems [10]. In their studies, behavior of magnetism whether antiferromagnetism or ferromagnetism is highly dependent on the presence of oxygen vacancies. Recently, Punnoose et al. [11] reported that SnO_2 doping with Fe by chemical method leads to ferromagnetism with a Curie temperatures of 850

K. To authors' knowledge, The strain and grain size effect Fe doping SnO_2 nanoparticles have not been studied much in literature. By doping of Fe^{2+} in SnO_2, it may introduce oxygen vacancy or trap level within band gap of SnO_2. Also, since particles are in nanosized range, surface/volume atomic ratio is large. This may alter grain size of pure SnO_2 and Fe^{2+} doped SnO_2 naoparticles.

In this paper, we have synthesized Fe^{2+} doped SnO_2 nanoparticles by co-precipitation method using stannous chloride and ferrous sulphate as a precursor, ammonia solution as a precipitating agent and carbon black powder as reducing agent. With this method, we can prepare SnO_2 nanoparticles in large amount with low cost precursors. Strain and crystallite size effect of Fe doping on SnO_2 nanoparticles are are studied.

2. Experimental

2.1 Chemicals

All chemicals used in the experiment are analytic reagent grade. Stannous chloride ($SnCl_2.2H_2O$) is purchased from Glaxo SmithKline Pharmaceutical Ltd. Ammonia solution (25 %), iron (II) sulphate heptahydarate GR and carbon black powder are purchased from Merck, India. All chemicals are used as received without further purification. Deionized water is used during the reaction.

2.2 Synthesis

In typical preparation of Fe doped SnO_2 (2 at. %), 2 g of stannous chloride dihydrate and 0.050 g iron sulphate are dissolved in 100 ml water. After complete dissolution, about 4 ml ammonia solution is added to above aqueous solution with stirring. Stirring is continued for 20 minutes. White gel precipitate is immediately formed. It is allowed to settle down for a night. Then it is filtered and washed with water 2-3 times. 0.252 g carbon black powder (charcoal activated) is mixed with filtered precipitate. The obtained mixer is dried for 24 h at 70 °C. Dried powder is grind and fired at 600 °C for 4 h. The procedure is repeated for 5 and 10 at. %.

2.3 Characterization

The powder x-ray diffraction (XRD) is performed using Philips Holland, XRD system PW 1710 with nickel filtered CuK_α (λ = 1.5405 Å) radiation. The average crystallite size (t) has been calculated from the line broadening using the Scherrer's relation: $t = 0.9\lambda/B\cos\theta$, where λ is the wavelength of x-ray and B is the half maximum line width. The transmission electron microscopy (TEM) is performed with Tecnai 20 G^2 under 200 KV. Samples are prepared by dispersing drop of colloid on copper grid, covered with the carbon film, and the solvent is evaporated. To record Fourier transform infra-red (FTIR) spectra, Bomem Hartmann & Brun MB Series Infrared spectrometer is used. SnO_2 powder is grind with KBr particles (1:5) and pressed into thin pellets.

3. Results and discussion

3.1 XRD study

XRD patterns of pure and Fe doped SnO_2 (2, 5 and 10 at. %) nanoparticles prepared at 600 °C is shown in Figure 1. All the peaks of XRD belong to tetragonal lattice of SnO_2. The lattice parameters are calculated by using program Unit Cell - method of TJB Holland & SAT Redfern 1995. The calculated lattice parameters of pure SnO_2 (x = 0) are a = 4.723(1) Å, c = 3.238(1) Å and its unit cell volume is V = 72.24 $Å^3$ and these values are well agreement with the reported values (JCPDS file No. 71-0652). The peaks are broad due to the nano-size effect. No trace of secondary phase is found. The unit cell volume increases slightly with Fe^{2+} doping indicating substitution of Sn^{4+} sites by Fe^{2+} ions. The unit cell volume increases from 72.24 to 72.90 $Å^3$ as Fe concentration varies from 0 to 10 at. %.

With increase of Fe^{2+} concentration, the peaks in x-ray diffraction pattern are becoming broad because of strain effect from substitution of lower ionic radius of Sn^{4+} (0.69 Å) by large one Fe^{2+} (0.77 Å) [12]. The lattice parameters for Fe doped SnO_2 (0, 2, 5 and 10 at. %) are given in Table 1.

The crystallite size decreases from 21 to 11 nm when Fe concentration varies from 0 to 10 at. %.

Table 1. Lattice parameters, unit cell volume and crystallite size of Fe doped SnO_2 (0, 2, 5, 10 at. %)

Fe concentration at. %	*a* (Å)	*c* (Å)	*V* (Å ^{3})	Crystallite size (nm)
0	4.723(1)	3.238(1)	72.24	21
2	4.720(1)	3.250(1)	72.40	17
5	4.731(1)	3.240(1)	72.55	13
10	4.747(1)	3.234(1)	72.90	11

Figure 2 shows the XRD patterns of the strongest peak (110) for Fe doped SnO_2 (0, 2, 5, 10 at. %) nanoparticles. Each data are fitted with Lorentzian equation. The peak maxima are at 2θ = 26.652, 26.585,

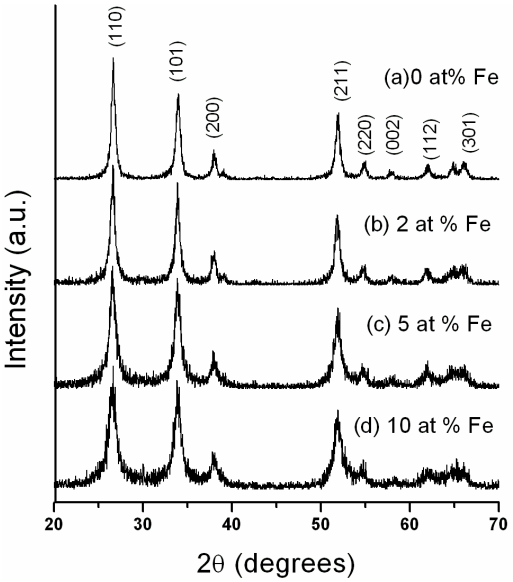

Fig. 1 XRD patterns of pure SnO_2 and Fe^{2+} doped SnO_2 nanoparticles. Dots indicate the fit to data using Lorentzian equation.

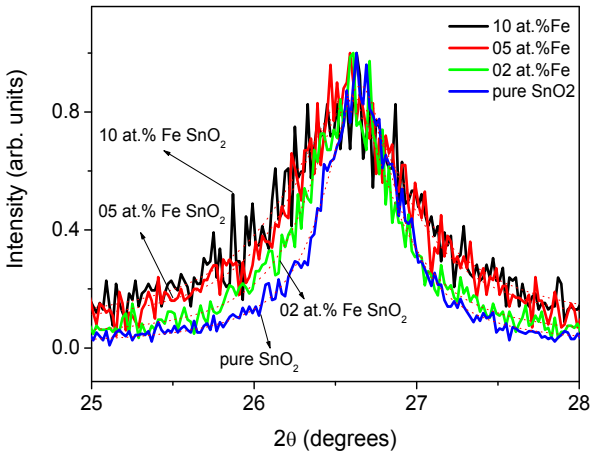

Fig. 2 XRD patterns of the strongest peak (110) for pure SnO_2 and Fe^{2+} doped SnO_2 nanoparticles.

26.582 and 26.572° for 0, 2, 5 and 10 at. % respectively. It indicates the expansion of unit cell volume with Fe^{2+} doping in SnO_2. This is contrary to the reported values in Fe doped SnO_2, where unit cell volume decreases with Fe^{2+} doping in SnO_2 [13].

3.2 TEM study

Figure 3 shows TEM micrograph of pure SnO_2 nanoparticles (scale 20 nm) prepared at 600 °C. The average grain size obtained from TEM microstructure is nearly 19 nm. It is slightly less than crystallite size obtained from XRD analysis (21 nm) using Scherrer's formula. Inset of Fig 3 shows its selected area electron diffraction (SAED) pattern. From this tetragonal patterns of spots are observed indicating the high crystallinity of sample.

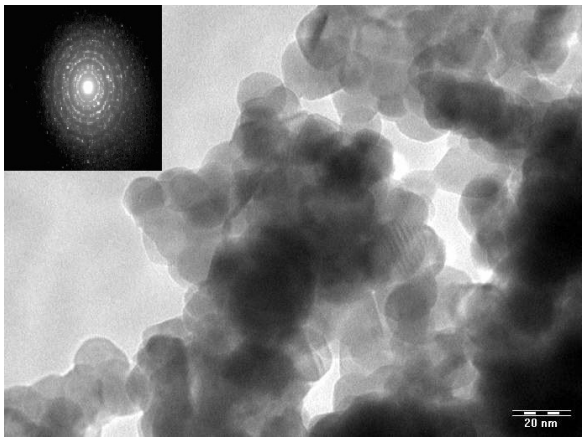

Fig. 3 TEM image of pure SnO_2 particles and 10 at. % inset shows its SAED patterns.

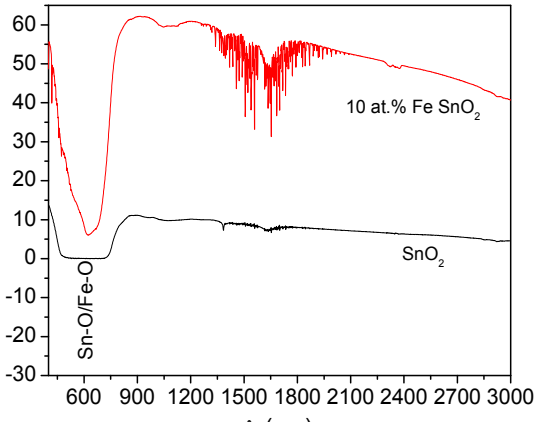

Fig. 4 IR spectrum of pure SnO_2 and Fe^{2+} doped SnO_2 nanoparticles.

3.3 FTIR study

FTIR spectra of pure SnO_2 and 10 at. % Fe doped SnO_2 nanoparticles prepared at 600 °C are shown in figure 4. The broad peak centered at 650 cm^{-1} is observed. It was reported that the broad band between 800 and 500 cm^{-1} were attributed to framework vibrations of Sn-O/Fe-O bond [14-16].

4. Conclusions

Fe^{2+} ions are doped into SnO_2 lattice successfully. Unit cell volume increases with Fe^{2+} ions incorporation in SnO_2. With increase of Fe^{2+} concentration, the peaks in x-ray diffraction pattern are becoming broad because of strain effect from substitution of lower ionic radius of Sn^{4+} (0.69 Å) by large one Fe^{2+} (0.77 Å). The crystallite size decreases from 21 to 11 nm when Fe concentration varies from 0 to 10 at. %.

Acknowledgments

One of authors (Amrut Lanje) wishes to acknowledge UGC, New Delhi, for financial support in present research work. Authors also thank to UGC-DAE Consortium for Scientific Research Center, Indore and Principal Dr. Ambedkar College, Chandrapur for providing Laboratory facilities.

References

A. S. Lanje, R. S. Ningthoujam, S. J. Sharma, R. B. Pode, R. K. Vatsa, (2010). Int. J. Nanotechnol.7, Nos. 9/10/11/12, 979.

Z.M. Jarzebski, J.P. Maraton, (1976). J. Electrochem. Soc. 123, 199.

V. Vasu, A. Subramanyan, (1990). Thin Solid Films 193–194, 973.

A. Tsunashima, (1986). J. Mater. Sci. 21, 2731.

C. Kilic, A. Zunger, (2002). Phys. Rev. Lett. 88, 095501.

M. Sawada, M. Higuchi, S. Kondo, Jpn. (2001), J. Phys. Part I 40, 3332.

C. Xu, J. Tamaki, N. Miura, (1991). Sens. Actuators B 147, 3.

A.L. Dawar, J.C. Joshi, (1984). J. Mater. Sci. 19, 1.

R. Janisch, P. Gopal, N. Spaldin, (2005). J. Phys.: Condens. Matter 17, R657.

J. Phys.: Condens. Matter 18 (2006) 6001.

A. Punnoose, J. Hays, A. Thuber, 2013M.H. Engelhard, R.K. Kukkadapu, C. Wang, V. Shutthanandan, S. Thevuthasan, (2005). Phys. Rev. B 72, 54402.

R. D. Shannon, C. T. Prewitt, (1969). Acta Crystallogr. B 25, 925.

J. Hays, A. Thurber, K. M. Reddy and A. Punnoose, (2007). Transworld Research Network 37/661 (2), Magnetism in semiconducting oxides.

R. S. Ningthoujam, V. Sudarsan, S. K. Kulshreshtha, (2007). J. Lumin. 127, 747.

R. S. Ningthoujam, D. Lahiri, V. Sudarsan, H. K. Poswal, S. K. Kulshreshtha, S. M. Sharma, B. Bhushan, M. D. Sastry, (2006). Mater. Res. Bull. 42, 1293.

A. S. Lanje, S. J. Sharma, R. S. Ningthoujam, J. -S. Ahn, R. B. Pode, (2013). Advanced Powder Technology 24, 331.